Trapped and precipitating protons in the inner magnetosphere as seen by IMAGE

J. D. Perez,[1] X.-X. Zhang,[1,2] P. C:son Brandt,[3] D. G. Mitchell,[3] J.-M. Jahn,[4] C. J. Pollock,[4] and S. B. Mende[5]

Received 4 February 2004; revised 17 May 2004; accepted 29 June 2004; published 4 September 2004.

[1] Images from the IMAGE satellite of precipitating protons (SU12/FUV) and trapped protons at 8.5 (MENA) and 33 keV (HENA) are compared during three periods: (1) 12 August 2000 from 1000 UT to 1145 UT just after the peak of a strong geomagnetic storm, (2) 2 June 2001 from 0100 to 0345 UT during the main phase and initial recovery of a weak storm, and (3) 18 June 2001 from 1400 to 1645 UT late in the recovery phase of another weak storm. Some of the features of the precipitating and trapped protons observed in these time intervals have been previously reported for other events, especially the fact that the strength of the precipitating protons and trapped protons do not always correlate. The primary new features are that (1) the fluxes of the precipitating protons and both the 8.5 keV and 33 keV trapped protons peak at similar magnetic latitudes and that (2) the peak in the 8.5 keV trapped protons is usually at the same MLT as the peak in the precipitating protons, while the peak in the 33 keV trapped protons is usually in a different MLT region than the peak of the precipitating protons. Some possible mechanisms to explain these observations are presented, but understanding this behavior should provide stringent tests for models of the Earth's inner magnetosphere. *INDEX TERMS:* 2720 Magnetospheric Physics: Energetic particles, trapped; 2716 Magnetospheric Physics: Energetic particles, precipitating; 2730 Magnetospheric Physics: Magnetosphere—inner; 2704 Magnetospheric Physics: Auroral phenomena (2407); 2776 Magnetospheric Physics: Polar cap phenomena; *KEYWORDS:* trapped protons, precipitating protons

Citation: Perez, J. D., X.-X. Zhang, P. C:son Brandt, D. G. Mitchell, J.-M. Jahn, C. J. Pollock, and S. B. Mende (2004), Trapped and precipitating protons in the inner magnetosphere as seen by IMAGE, *J. Geophys. Res.*, *109*, A09202, doi:10.1029/2004JA010421.

1. Introduction

[2] The SI12/FUV instrument [*Mende et al.*, 2000] on board the IMAGE satellite [*Burch*, 2000] has provided the first images of the aurora that distinguish precipitating protons from electrons. The state of our knowledge of the proton aurora prior to the SI12/FUV measurements was summarized by *Mende et al.* [2001]. In general the proton aurora is collocated with the diffuse electron precipitation, and it is on closed field lines. During the growth phase of substorms, the proton aurora moves equatorward with the development of the ring current. In the premidnight sector the proton aurora is not part of the leading edge of the poleward expansion of the auroral bulge, and the diffuse proton aurora lies equatorward of the discrete aurora. At onset the poleward boundary of the proton aurora reaches almost as far poleward as the electron aurora, but the westward surge does not contain proton aurora. The proton arc is always equatorward of the electron arc but somewhat less so at midnight. The proton aurora expands poleward to occupy a large, diffuse region poleward of the presubstorm position. The electron arc that brightens lies within the proton precipitation region. From a statistical study, it is shown that in the postmidnight and dawn local time regions, the precipitating protons are poleward of the electrons [*Mende et al.*, 2003]. The energy of the precipitating protons decreases with decreasing latitude.

[3] The first SI12/FUV proton auroral images were reported by *Mende et al.* [2001] for a substorm on 28 June 2000 in the time period 1956–2049 UT with onset at approximately 2000 UT. The first sign of electron breakup preceded the proton response by 4 min. Some of the proton precipitation reached higher latitude than the bright electron surge, but the proton intensification occurred at the original location of the proton aurora. Later, electrons were brightest at the poleward edge of the surge, while protons were brightest equatorward and westward. The protons seemed to drift westward and electrons eastward as expected. The protons were energized by electric fields well inside the magnetosphere in the region of geosynchronous orbit.

[4] Subauroral, detached arcs that are perhaps associated with an eroded plume of the plasma sphere have been

[1]Physics Department, Auburn University, Auburn, Alabama, USA.
[2]Currently at Alabama A & M University, Normal, Alabama, USA.
[3]Applied Physics Laboratory, Johns Hopkins University, Laurel, Maryland, USA.
[4]Southwest Research Institute, San Antonio, Texas, USA.
[5]Space Science Laboratory, University of California, Berkeley, California, USA.

0148-0227/04/2004JA010421

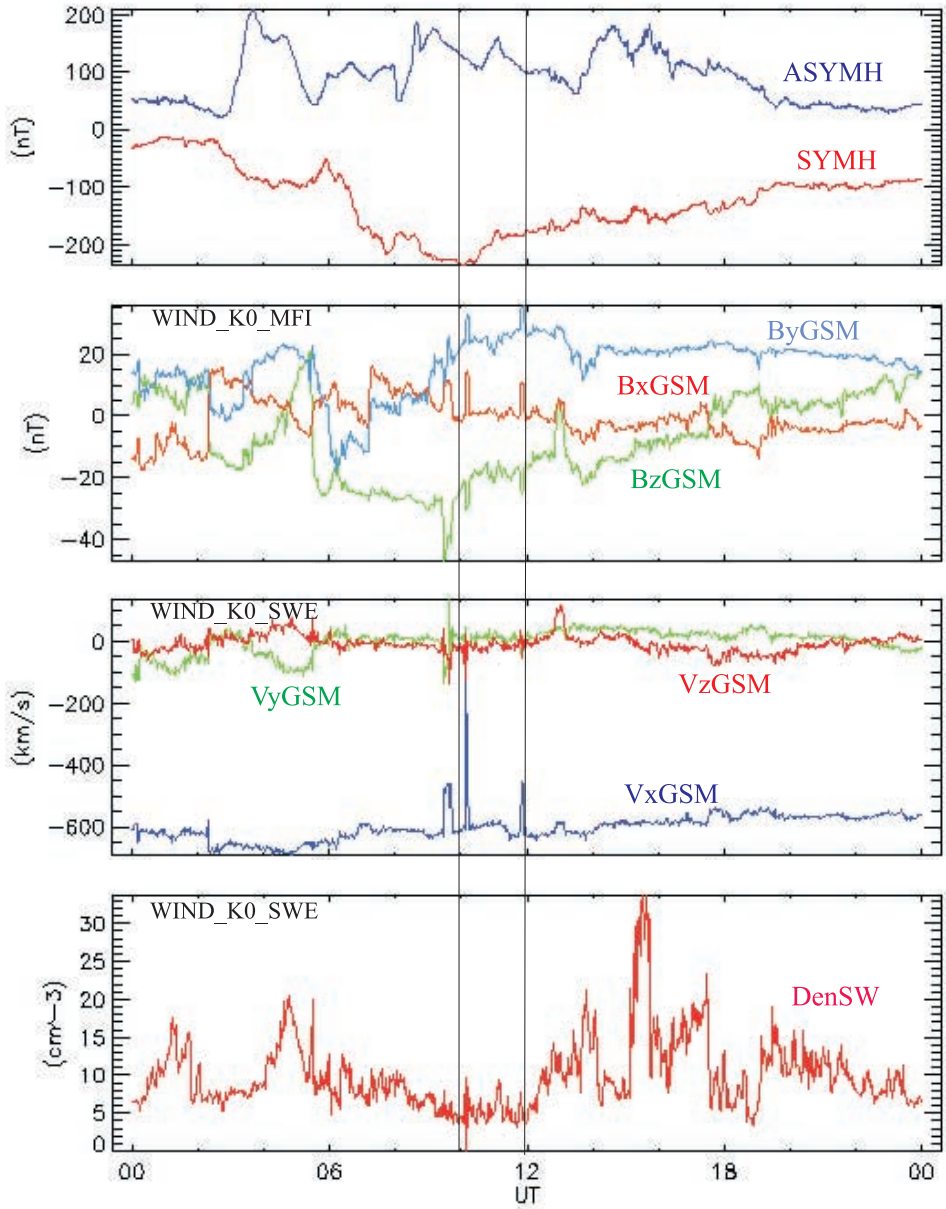

Figure 1. Geomagnetic activity indices and solar wind parameters for 12 August 2000. The vertical lines show the time period, 1000–1145 UT, of interest in this paper.

observed by SI12/FUV in the afternoon sector on 9–10 November 2000, 2339–0057 UT and 23 January 2001, 2259–2459 UT [*Burch et al.*, 2002; *Immel et al.*, 2002]. On 9–10 November 2000, when B_z turned northward, the auroral oval moved poleward, leaving a detached arc in the afternoon sector. AE was decreasing, so it was the recovery phase of the substorm. The ring current was not active, and the detached arc did not move. Comparison with HENA/ENA images for 10–60 keV neutrals showed neutrals at midnight, while proton precipitation was in the postmidnight/predawn and postnoon/predusk sectors. On 23 January 2001, the phenomenology was similar except B_y changes from negative to positive. Again HENA/ENA images showed neutral atom emission in the postmidnight/predawn sector. Using FAST [*Carlson et al.*, 2001] data, *Immel et al.* [2002] showed that the precipitating protons had energies in the 20–35 keV range.

[5] During observation of a substorm recovery phase aurora on 11 June 2000, 1515–1538 UT [*Mende et al.*, 2002a], WIC/FUV images showed a double aurora. The equatorward part was both proton aurora and diffuse electrons with embedded structures. Poleward after the gap, the arc was primarily electrons.

[6] *Mende et al.* [2002b] compared (1) trapped proton flux as evidenced by 16–27 keV HENA ENAs without mass resolution and (2) proton precipitation as shown by SI12/FUV. Both were integrated over space. Prior to a substorm, levels of both were quite similar. Just prior to onset, trapped particles increased while precipitation decreased. Then in response to the substorm as detected

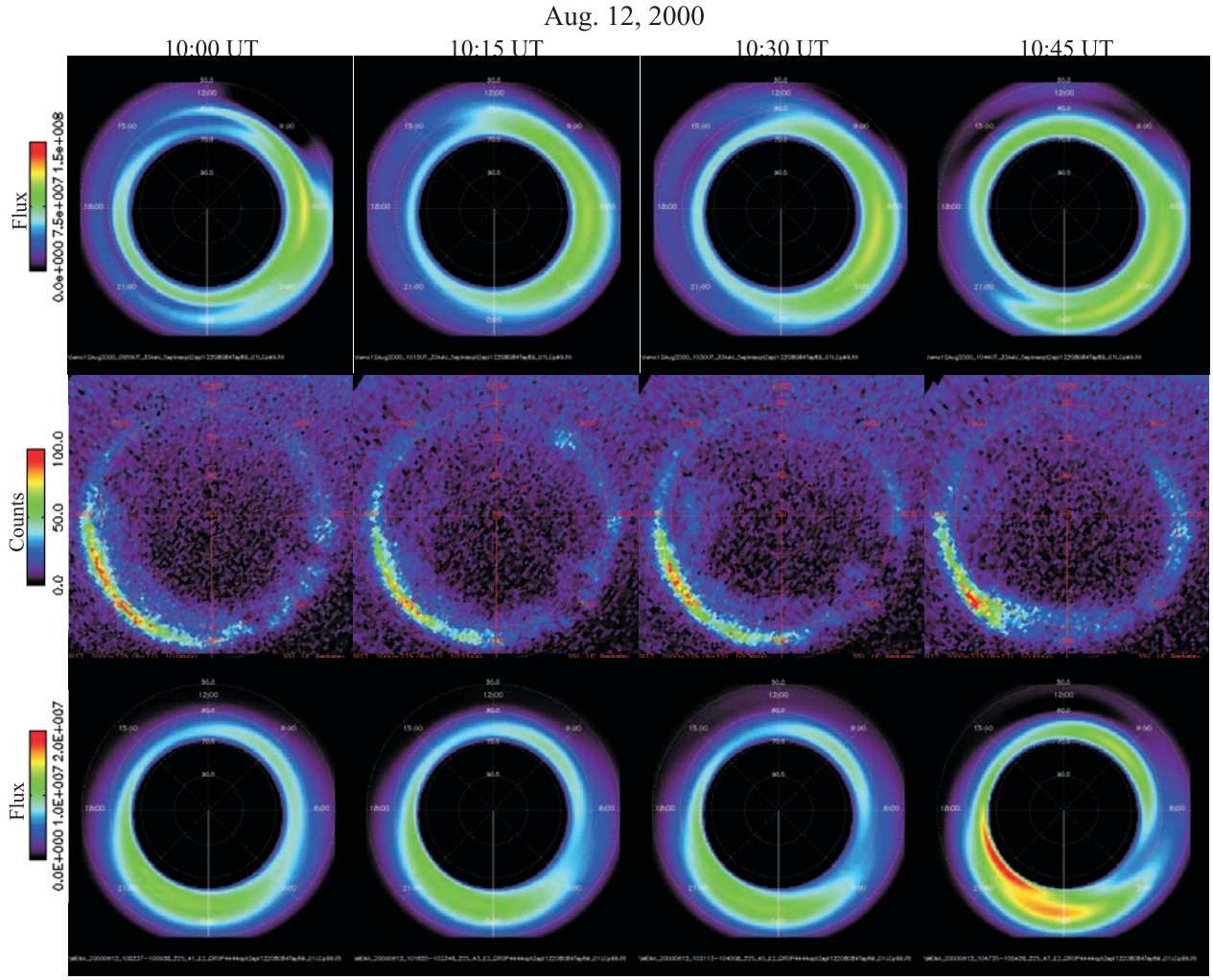

Figure 2. Images from 1000–1045 UT on 12 August 2000. Top and bottom row are trapped proton flux mapped to the northern ionosphere from equatorial distributions integrated over pitch angles deconvolved from ENA images from HENA and MENA, respectively. Middle row are precipitating protons as seen by SI12/FUV. Noon is up. Circles show magnetic latitude in 10° intervals.

in the WIC/FUV images, the trapped flux rose more slowly than precipitating flux.

[7] In this paper, proton precipitation as observed by SI12/FUV is directly compared with the trapped proton flux as deconvolved from MENA (5–12 keV) [*Pollock et al.*, 2000] and HENA (27–39 keV) [*Mitchell et al.*, 2000] neutral atom images for three periods of time. The three events are (1) 12 August 2000 from 1000 UT to 1145 UT, just after the peak of a strong geomagnetic storm, (2) 2 June 2001 from 0100 to 0345 UT, during the main phase and initial recovery of a weak storm, and (3) 18 June 2001 from 1400 to 1645 UT, late in the recovery phase of another weak storm. The images are described in section 2, and the implications of the observations are discussed in section 3. Section 4 contains a summary and conclusions.

2. Observations

[8] In this section a series of images from HENA (27–39 keV), SI12/FUV, and MENA (5–12 keV) are displayed at 15 min intervals for time periods during three geomagnetic storms in which it was possible to obtain meaningful images from all three instruments. The middle row in each figure shows the proton precipitation images from SI12/FUV. The response of this instrument is strongly dependent on the flux of charge exchange protons (hydrogen) moving away from the observer with a velocity of at least that of 2 keV protons. So precipitating protons that are clearly above this threshold, say at 8 keV, would be detected with approximately the same efficiency as protons at 33 keV. The images have a 2 min time resolution. The first and third rows of each figure show trapped proton fluxes derived from HENA and MENA energetic neutral atom images (ENA), respectively. First the ENA images are deconvolved to obtain equatorial pitch angle distributions of trapped protons [*Perez et al.*, 2000; *Perez et al.*, 2001]. It is to be noted that in order to obtain the results shown, a minimum uncertainty for the pixels in the ENA images with small fluxes were chosen to reduce the importance of "fitting" those pixels. The equatorial fluxes were then integrated

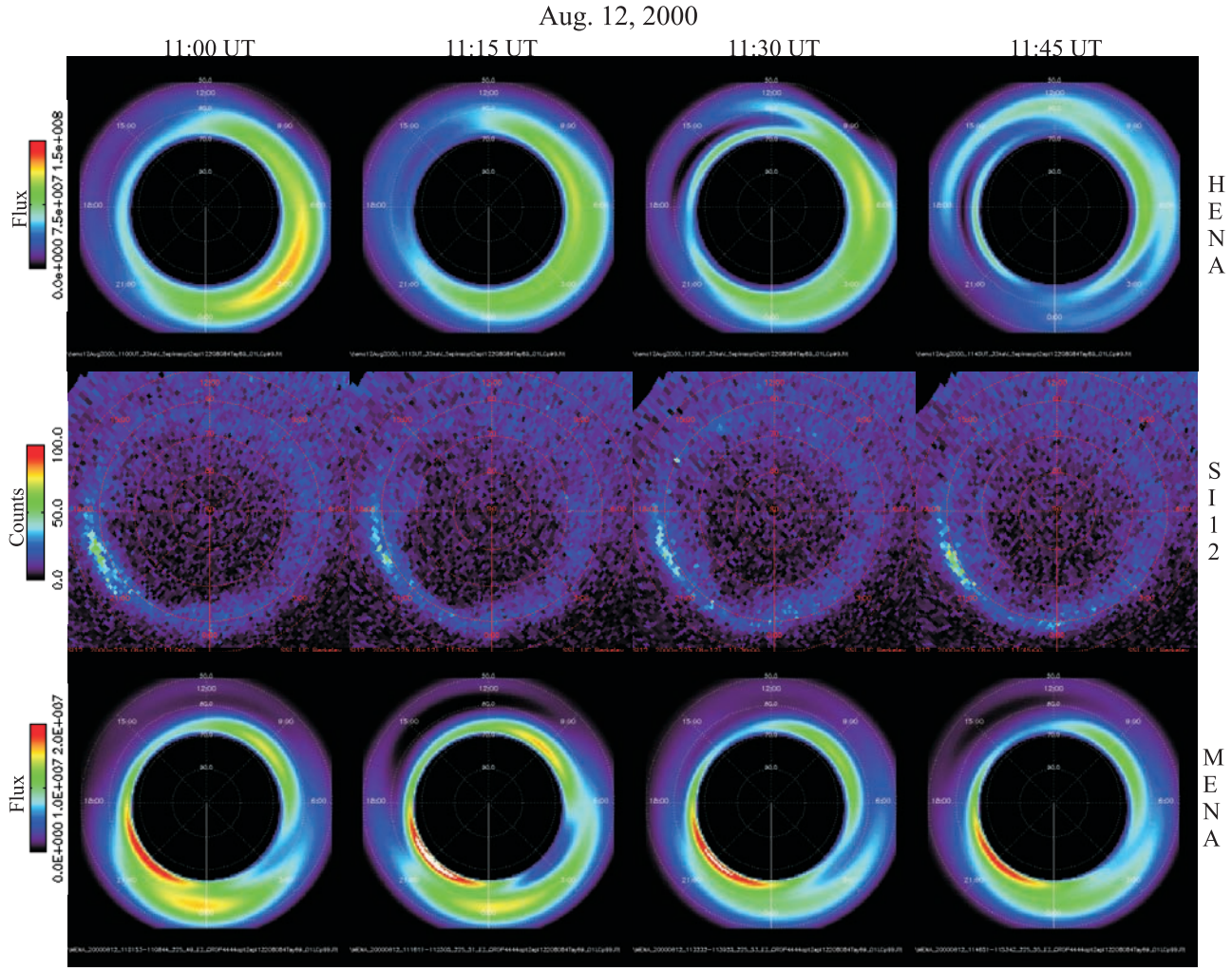

Figure 3. Images from 1100–1145 UT on 12 August 2000. Format is the same as Figure 2.

over pitch angle and mapped along magnetic field lines to the northern polar ionosphere. The Tsyganenko89 magnetic field model is used [*Tsyganenko*, 1989]. No calculations of expected precipitation from the trapped population have been performed. The observed trapped population is mapped for direct comparison with the observed precipitation. The ENA images are integrated over 8–10 min.

[9] In all the images, noon is at the top, dawn is to the right, dusk is to the left, and midnight is at the bottom. Magnetic latitudes from 50° to 90° are shown in 10° intervals. The color bars are different for each instrument but the same for all times for a particular event.

2.1. Strong Storm Early Recovery Phase on 12 August 2000

[10] The top panel in Figure 1 shows the geomagnetic indices SYMH, a proxy for Dst, and ASYMH, a proxy for AE, on 12 August 2000. It is seen that this is a large storm, minimum SYMH was approximately −250 nT and that the time period in which the precipitating and trapped proton fluxes are compared in this paper, 1000–1145 UT, encompasses the first 2 hours of the recovery phase. There is a peak in ASYMH at approximately 1100 UT. The WIND satellite was far out on the dawnside just behind the Earth, so there is no need for a time shift for the solar wind parameters shown in the remaining three panels. During the time period of interest, B_z is strongly negative. B_y is strongly positive. The solar wind velocity and density remain fairly steady at ∼500 km/s and 5 cm^{-3}, respectively.

[11] The trapped and precipitating proton fluxes are shown in Figures 2–3 at 15 min intervals from 1000 to 1145 UT. In Figure 2 the precipitating proton counts peak in the postdusk/premidnight sector near 2100 MLT at approximately 55° magnetic latitude. The precipitation occurs over approximately a 5° width. The 8 keV trapped protons also peak in the postdusk/premidnight sector but at somewhat larger magnetic latitude, i.e., approximately 60°. The spread is also larger, i.e., closer to 10°. The 33 keV trapped protons peak near dawn at approximately 60° magnetic latitude with a spread of approximately 10°. At 1045 UT, just prior to a peak in the ASYMH index, a second peak in the trapped proton flux appears in the 8 keV energy band at higher latitude and earlier in MLT. The 33 keV peak moves into the postmidnight/predawn sector at somewhat lower latitude.

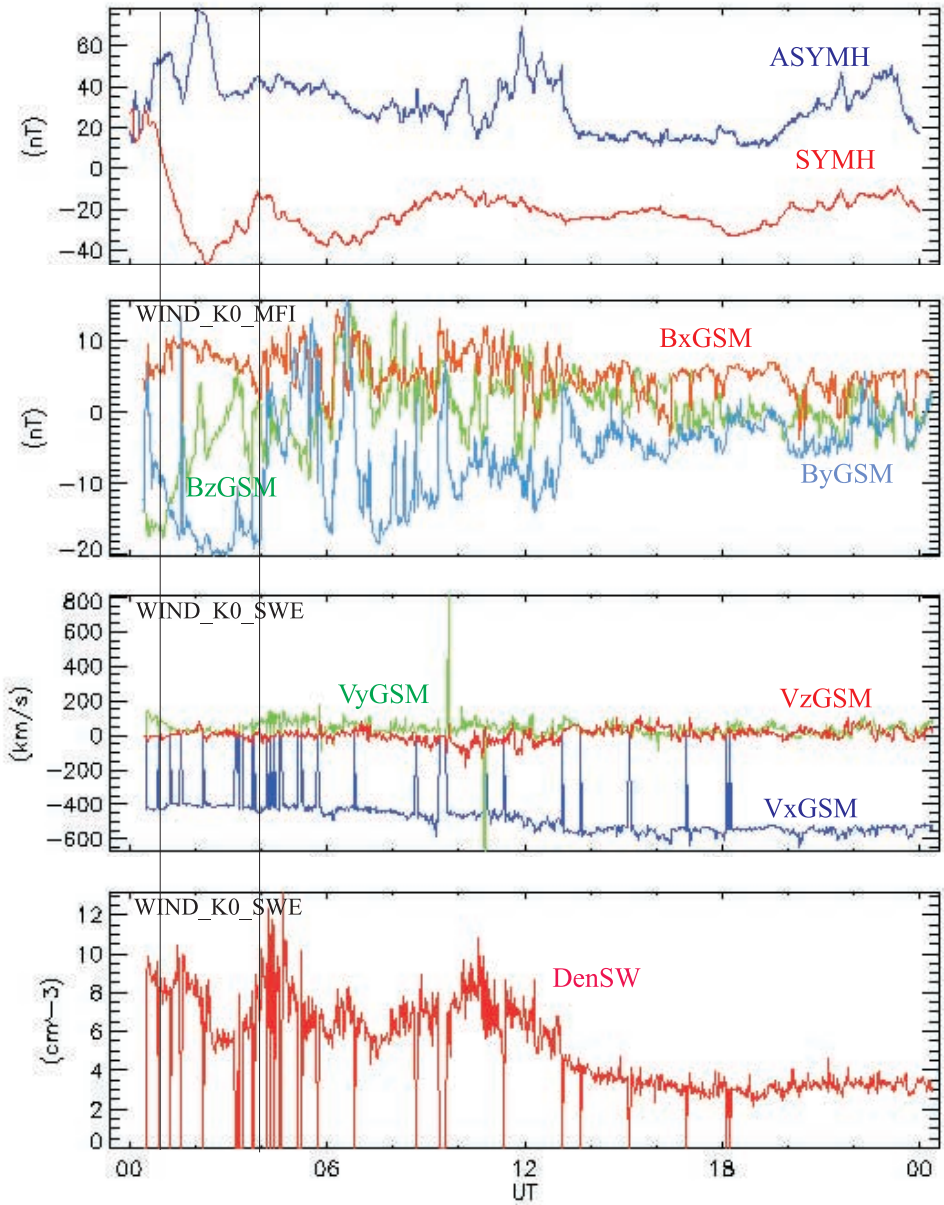

Figure 4. Geomagnetic activity indices and solar wind parameters for 2 June 2001. The vertical lines show the time period, 0100–0345 UT, of interest in this paper.

[12] In Figure 3 the flux of precipitating protons between 1100 UT and 1145 UT decreases, showing no response to the peak in ASYMH at 1100 UT. The postdusk/premidnight 8 keV trapped proton peak brightens then diminishes slightly while the peak near midnight diminishes in intensity. The peak in the 33 keV trapped protons brightens at 1100 UT but then dims and moves back to dawn and to higher latitude.

2.2. Main Phase and Early Recovery of Weak Storm on 2 June 2001

[13] The top panel of Figure 4 shows the geomagnetic activity for a weak storm on 2 June 2001. The minimum in SYMH, −45 nT, occurs just after 0200 UT. During the time period, 0100–0345 UT, in which precipitating and trapped proton images are presented, there are two weak peaks in ASYM, one at 0100 UT and another at 0200 UT. Because of the position of the WIND satellite in front of the Earth, the solar wind parameters are shifted by 25 min. The solar wind B_z oscillates between negative and positive values, with positive peaks at approximately 0200, 0315, and 0345 UT. B_y is strongly negative until just after 0400 UT. The solar wind speed stays steady at just over 400 km/s, and the density has a peak at ~0130 UT.

[14] When SYMH goes negative at approximately 0100 UT, Figure 5 shows that the proton precipitation is strongest in the postdusk/premidnight sector. Then a peak develops postmidnight at the same magnetic latitude, i.e.,

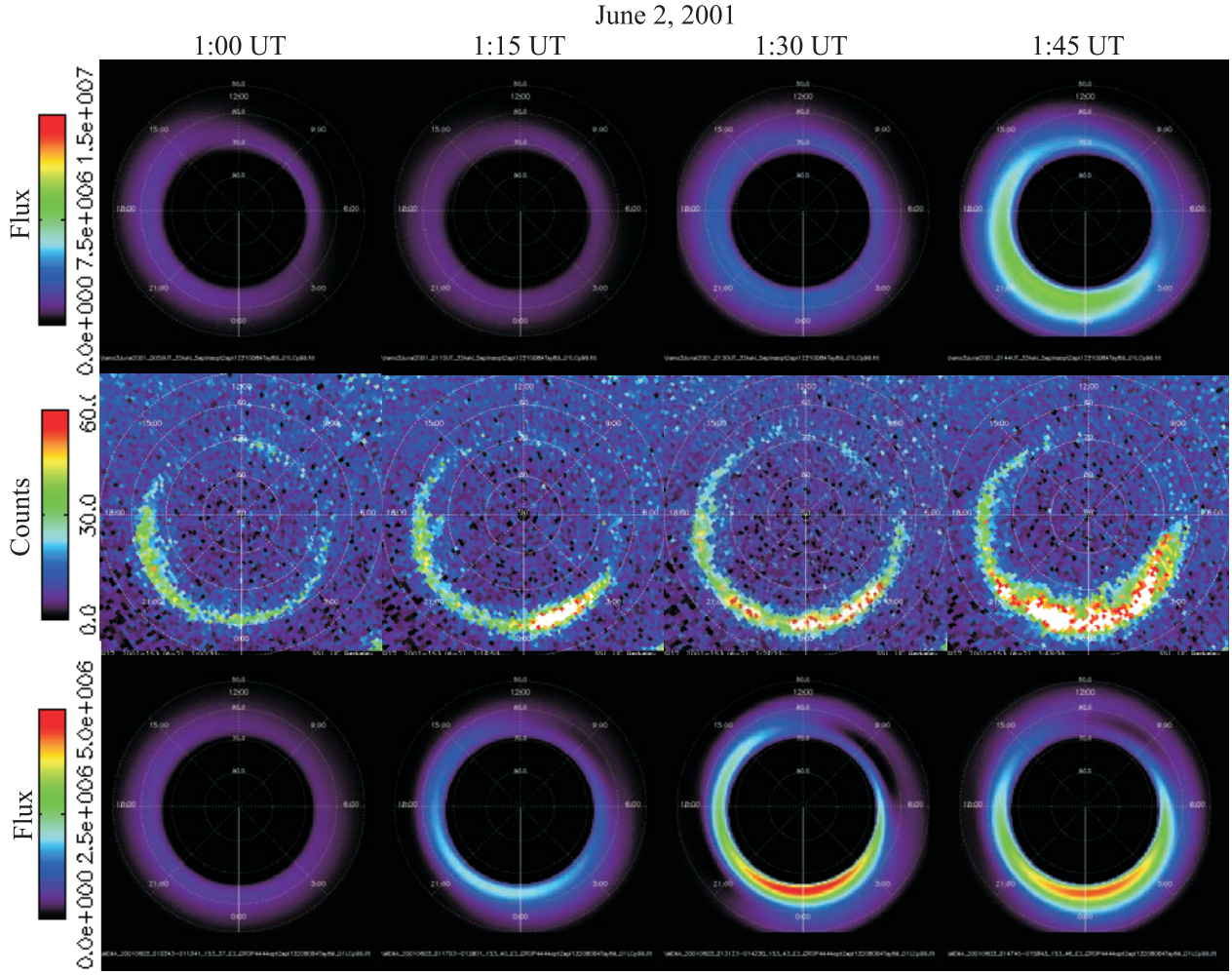

Figure 5. Images from 0100–0145 UT on 2 June 2001. Format is the same as Figure 2.

between 60° and 65°. At 0145 UT, the proton precipitation reaches a maximum across almost the entire nightside. The 8 keV trapped protons also brighten significantly at about the same time and location. The 33 keV trapped protons also increase in number at the same time and magnetic latitude but more toward dusk than the 8 keV trapped and the precipitating protons.

[15] During the next hour, Figure 6 shows that at 0200 UT, the number of precipitating protons diminishes postmidnight leaving a peak premidnight at ~60° magnetic latitude. For the remainder of the hour as SYMH increases, the counts decrease in the premidnight sector, producing again a peak postmidnight. The peak in the 33 keV trapped protons diminishes and moves to dusk during this hour. The peak in the 8 keV trapped protons also dims, but it stays near midnight.

[16] As SYMH continues to increase during the next hour, Figure 7 shows proton precipitation at ~65° on the nightside and more poleward at ~65°–70° in the postnoon/predusk sector, leaving a gap in the postdawn/prenoon sector. At 0345 UT the proton precipitation intensifies on the nightside prior to midnight. The 8 keV trapped protons strengthen but remain almost symmetrical with a gap also in the postdawn/prenoon sector. The latitude of the 8 keV trapped particles also moves poleward in the afternoon sector but not as much as the precipitating protons. The 33 keV trapped protons also increase in number, but while the peak is also at approximately 65°, it is on the duskside with a gap in the postmidnight/predawn sector.

2.3. Late in the Recovery Phase of a Weak Storm on 18 June 2001

[17] The storm on 18 June 2001 has its minimum SYMH at 0800 UT as shown in Figure 8. So by the time the IMAGE satellite is in position to provide good images, 1400 to 1645 UT, the storm is well into the recovery phase. During this period there is a peak in ASYMH at ~1500 UT. At the beginning of this period, B_z is negative, but at ~1500 UT, it goes positive. B_y is mainly positive with brief negative excursions just after 1400 UT until it swings negative at approximately 1600 UT. The solar wind velocity is steady at approximately 350 km/s, and the density is high, i.e., >30 cm^{-3}.

[18] Figure 9 shows, between 1400 and 1445 UT, a slight brightening of the precipitating protons that extends from dusk to past midnight at ~60° magnetic latitude. The

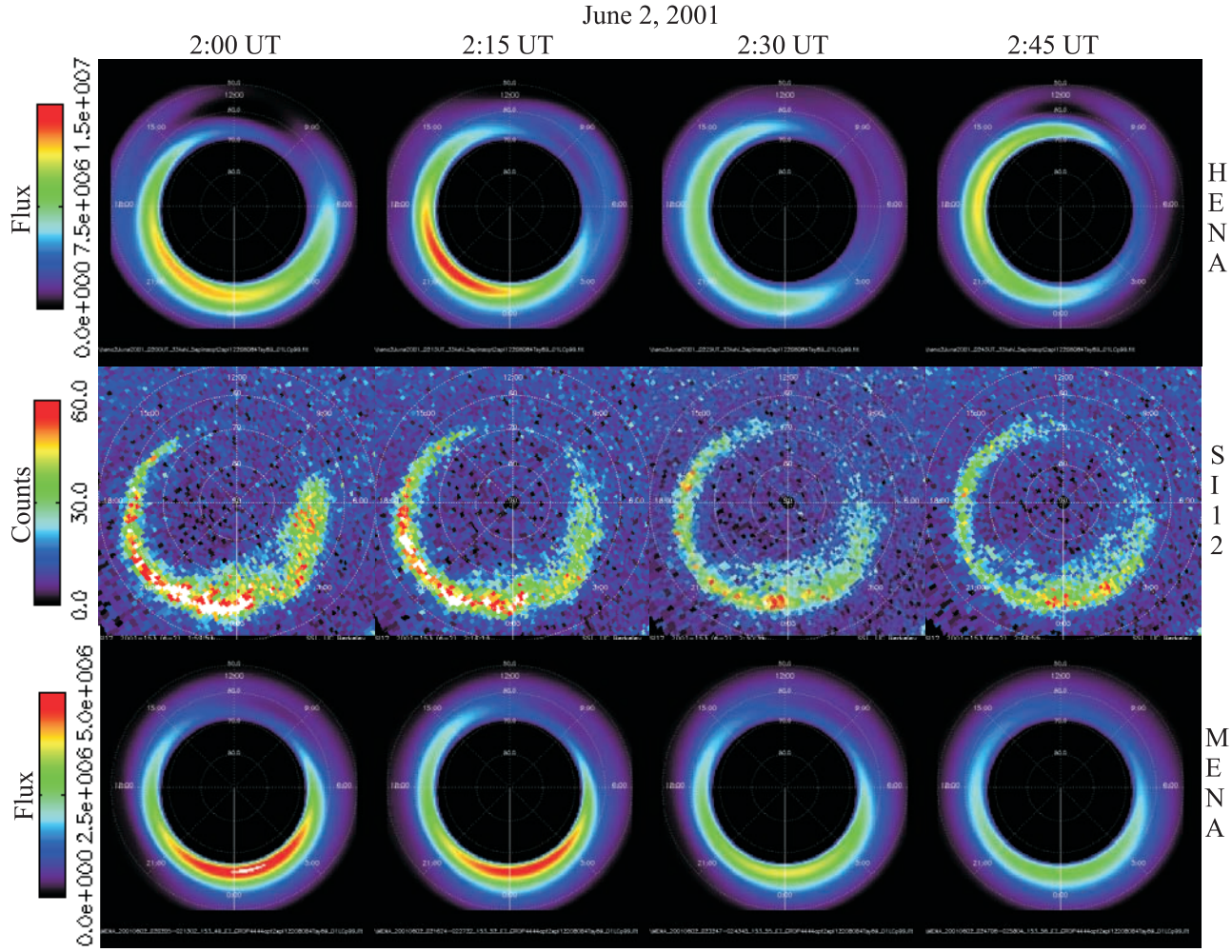

Figure 6. Images from 0200–0245 UT on 2 June 2001. Format is the same as Figure 2.

trapped protons remain at relatively low levels, with the 33 keV flux stronger on the dayside and the 8 keV flux higher on the nightside. The high-energy trapped protons are broad in magnetic latitude and are centered at 60°. The lower-energy trapped protons are narrow in magnetic latitude and are between 60° and 65°. At 1430 UT the 33 keV trapped protons show a short-lived peak in the postdusk/premidnight sector at ~60°.

[19] From 1500 to 1545 UT, as shown in Figure 10, the precipitating proton counts remain about the same. The view of the SI12/FUV instrument now is less obscured on the dawnside, and it shows that the precipitating proton flux extends to nearly 0300 MLT. The 33 keV trapped protons show a fairly symmetrical ring current between 60° and 70° magnetic latitude. The relatively weak peak remains on the dayside oscillating from postnoon to prenoon. The 8 keV trapped protons are also nearly symmetrical except for a gap near dusk. The peak is in the postmidnight/predawn sector at ~65° magnetic latitude.

[20] From 1600 to 1645 UT the precipitating protons remain weak and steady as shown in Figure 11. The 33 keV trapped protons now cover the entire dayside between 60° and 70° with a weak oscillation in the intensity. The 8 keV trapped protons remain nearly symmetrical with a gap near dusk.

3. Discussion

[21] In order to properly interpret the results presented in the previous section, it is essential to understand some of the uncertainties involved in obtaining the trapped proton images. The images obtained by SI12/FUV are direct observations of emissions produced by precipitating protons. Only minor uncertainties about the energy dependence of the production of the observed photons could influence the interpretation of the results presented here. On the other hand, the images of the trapped protons are derived results. They begin with ENA images. For HENA, the ENA images are composed of pixels that are nominally 6° × 6°, but the actual spread may be closer to 20°, and for MENA, the pixels are nominally 4° by 5°. but there is the possibility of blooming when the flux is high. For the ENA images presented in this paper, the satellite was at approximately 7 R_E giving a 4° pixel a width of 0.5 R_E at the equator. There are then a number of steps in the process that produces equatorial pitch angle distributions from the

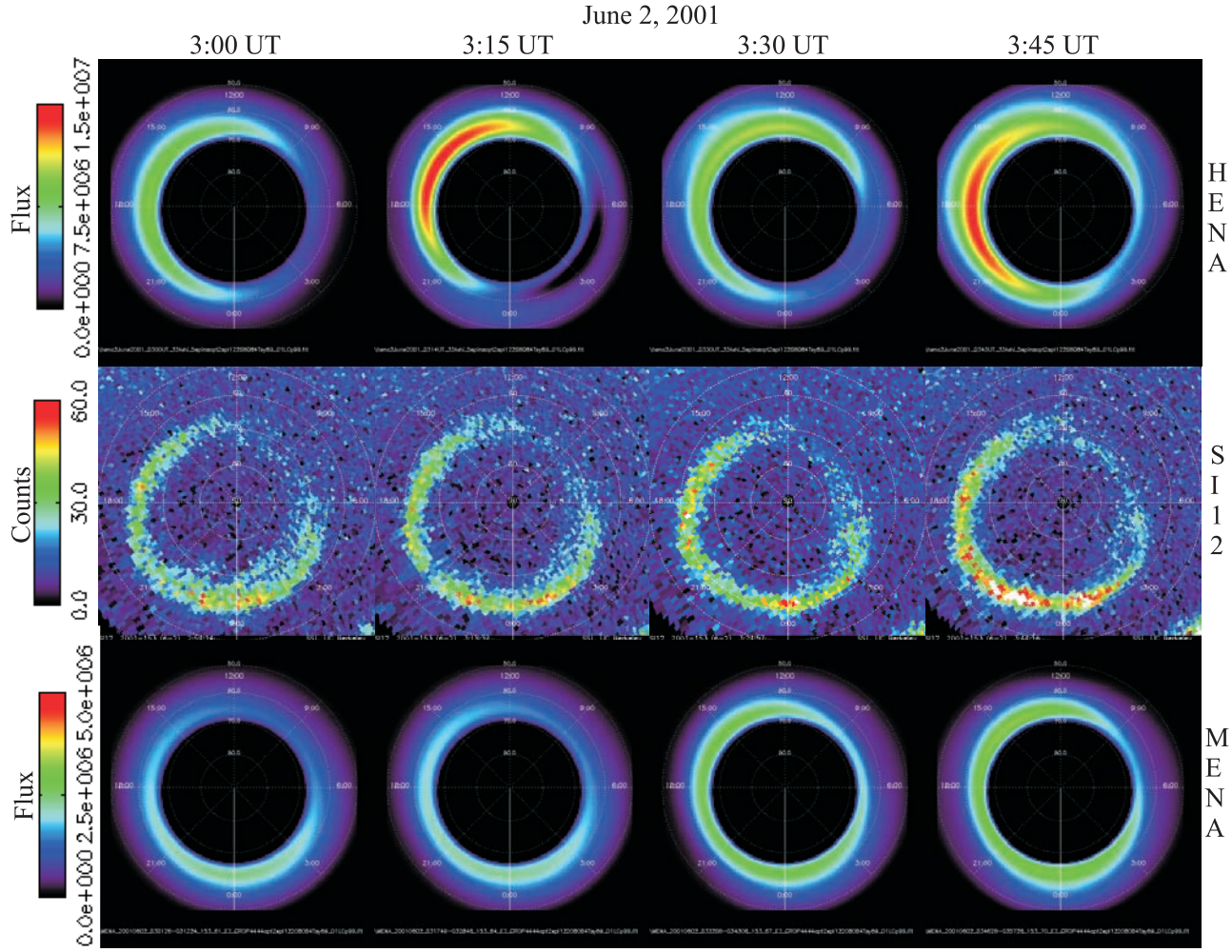

Figure 7. Images from 0300–0345 UT on 2 June 2001. Format is the same as Figure 2.

ENA images that also lead to uncertainties in addition to this basic instrumental effect. These are summarized by *Perez et al.* [2004]. Of particular note here is the fact that the ENA images are produced by the interaction of the trapped protons with the neutral hydrogen in the geocorona and the neutral oxygen in the exosphere. The decay of the neutral hydrogen density with distance from the Earth, a factor of 2.4 between 3.0 and 4.0 R_E [*Ostgaard et al.*, 2003], and the limitation of the neutral oxygen to altitudes below 1000 km mean that neutrals can be produced and observed to come from locations distant from the mapped equatorial position of the deconvolved proton distribution. Mapping the equatorial fluxes from the equator to the polar ionosphere is done using a magnetic field model, but this introduces little additional uncertainty, since the peaks in the trapped proton fluxes occur on field lines that are very nearly dipolar. It is not possible to rigorously combine these effects to determine a quantitative uncertainty for the magnetic latitude location of the trapped protons. Nevertheless, to provide some estimate, it can be noted that an uncertainty of 1 R_E at the equator introduces an uncertainty of 5° in magnetic latitude around 60° (L = 4 R_E). Given the position of the satellite above the pole and the fact that mapping along dipole field lines does not change MLT, the uncertainty in MLT is thought to be small enough that it does not affect any of the conclusions drawn in this paper.

[22] Some of the features to be noted in the observations presented here have been reported in other events. *Mende et al.* [2001] reported that the proton precipitation is on closed field lines. Given the very similar magnetic latitude of the precipitating and trapped protons, that is certainly the case for the three time periods in this paper. In the 12 August 2000 storm, it is seen that the proton precipitation does not follow the 1100 UT peak in the ASYMH index indicative of substorm activity, but the trapped particle flux does [*Mende et al.*, 2001]. Also on 12 August 2000, when B_z turns positive, the precipitating proton images show a detached arc in the afternoon sector and the cusp is visible, while the 33 keV trapped protons are brightest in the postmidnight/predawn sector with a gap in the postnoon/predusk sector similar to what has been reported during a number of other storms [*Frey et al.*, 2002; *Burch et al.*, 2002]. On the other hand, the time-dependent brightening of the 33 keV trapped protons at this time is indicative of activity in the ring current which is different than was reported by *Burch et al.* [2002].

[23] The first new feature reported here is that the precipitating protons and both the 8.5 keV and 33 keV

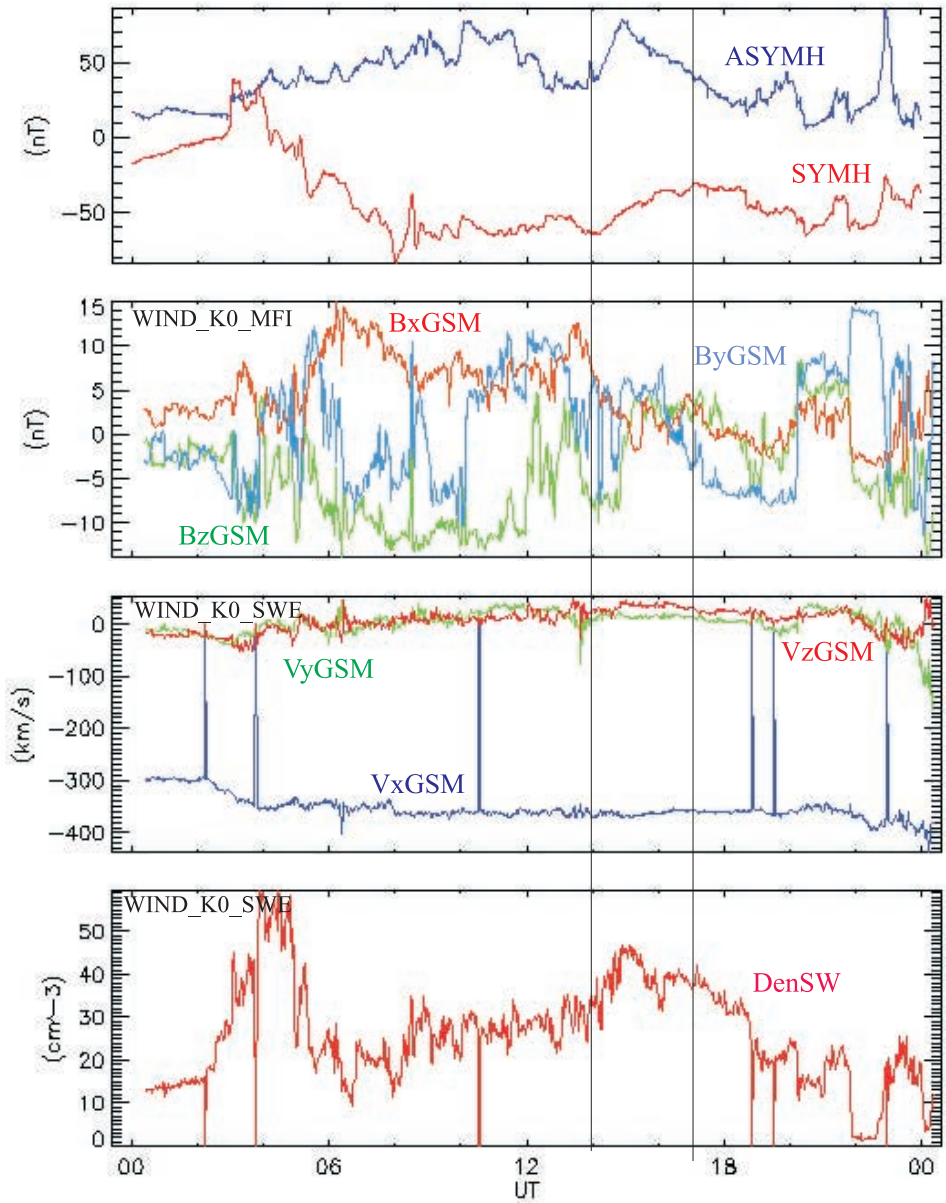

Figure 8. Geomagnetic activity indices and solar wind parameters for 18 June 2001. The vertical lines show the time period, 1400–1645 UT, of interest in this paper.

trapped protons peak at similar magnetic latitudes. A particularly good example is shown in the images at 0145 UT on 2 June 2001 (see Figure 5). The peak in the precipitating protons is centered around midnight between 60° and 65° magnetic latitude. In the postdusk/premidnight region, the magnetic latitude extent of the precipitating protons narrows with the peak very near 65°. Predusk, the weaker peak in the precipitating protons moves to higher magnetic latitude, i.e., approximately 65°. In the postmidnight/predawn sector, the precipitating protons move to higher magnetic latitude reaching 70°. Both the 8.5 keV and 33 keV trapped protons show almost identical variations with magnetic latitude. Within the uncertainties of the mapped magnetic latitude of the trapped protons, this feature is seen in all the images shown. This strongly suggests that the three populations, the precipitating protons, and the 8.5 keV and 33 keV trapped protons have a common origin.

[24] The fact that the strength of the precipitating protons and trapped protons do not correlate suggests, however, different origins for the three populations. This feature was reported by *Mende et al.* [2002b], using analysis of precipitating and trapped flux integrated over space. Examples shown here include (1) the rise of the trapped proton flux at both 8.5 keV (1045 UT, Figure 2) and 33 keV (1100 UT, Figure 3) on 12 August 2000, while the intensity of the precipitating protons is decreasing, and (2) the intensity of the precipitating protons on 18 June 2001 between 1400 UT (see Figure 9) and 1545 UT (see Figure 10) remains fairly steady while the flux of 33 keV protons is significantly

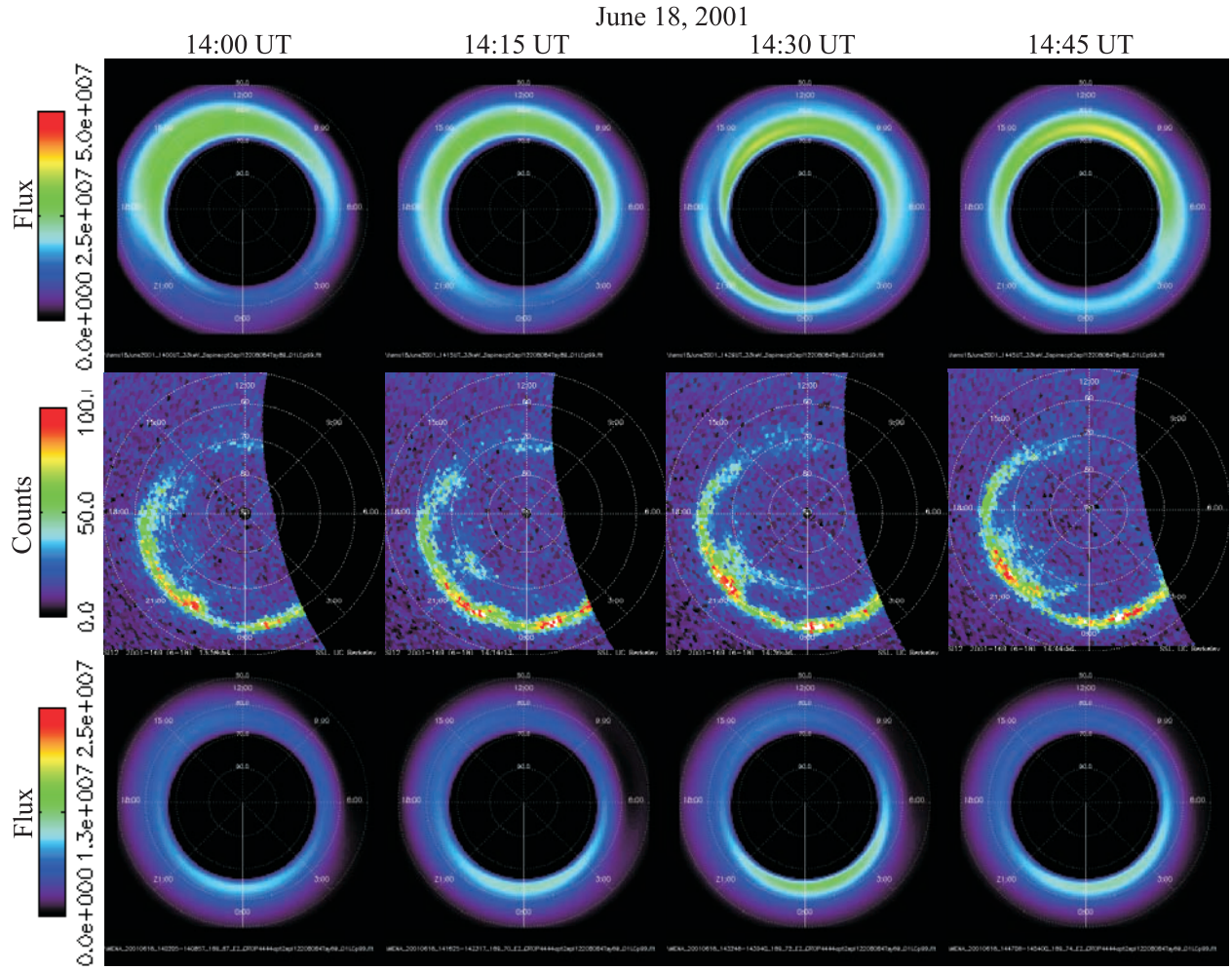

Figure 9. Images from 1400–1445 UT on 18 June 2001. Format is the same as Figure 2.

higher between 1515 UT and 1545 UT (see Figures 9 and 10) and the 8.5 keV flux remains fairly steady. A counter-example occurs between 0100 UT and 0145 UT on 2 June 2001 (see Figure 5), where the fluxes of all three seem to rise together.

[25] The second and most striking new feature demonstrated in the images shown in this paper is that the peak in the 8.5 keV trapped protons is usually at the same MLT as the peak in the precipitating protons, while the peak in the 33 keV trapped protons is usually in a different MLT region than the peak in the precipitating protons. The only counter-examples are for the weak storm on 2 June 2001 (see Figures 5–7), particularly during the main phase.

[26] The explanation for this last feature of the observations is difficult to pin down. The precipitation of the protons presumably occurs because trapped protons are pitch angle scattered into the loss cone. While there are two primary mechanisms for this pitch angle scattering, convection due to electric fields and wave-particle interactions [*Kozyra et al.*, 1997], observations [*Sóraas et al.*, 1999] and simulations [*Jordanova et al.*, 2001] suggest that particle interactions with electromagnetic ion cyclotron (EMIC) waves are the dominant mechanism. The question is whether there is an energy dependence in the wave particle interaction that favors either the 8.5 keV or the 33.0 keV trapped protons.

[27] One might argue that if the mechanism for pitch angle scattering into the loss cone is the interaction of the particles with fluctuating electric and magnetic fields, it would favor the lower-energy particles because it requires less force to move them into the loss cone. Indeed, *Erlandson and Ukhorskiy* [2001] found the simultaneous occurrence of EMIC waves with protons of energy 0.2–17.0 keV in the loss cone during magnetic storms. Observations using FAST [*Carlson et al.*, 2001] data, however, showed precipitating protons with energies in the 20–35 keV range [*Immel et al.*, 2002], and *Yahnin et al.* [2002] found precipitating protons in both the energy ranges 30–80 keV and <20 keV associated with EMIC waves.

[28] Another possibility is that the strong EMIC waves in the nightside interact more strongly with the 33.0 keV protons, causing strong precipitation but leaving their trapped distribution more pancake-like and therefore invisible to HENA when it is above the pole. It is not clear, however, why the EMIC waves would not also scatter the protons with pitch angles near 90 degrees to lower pitch angles, i.e., moving the distribution function toward isotropy.

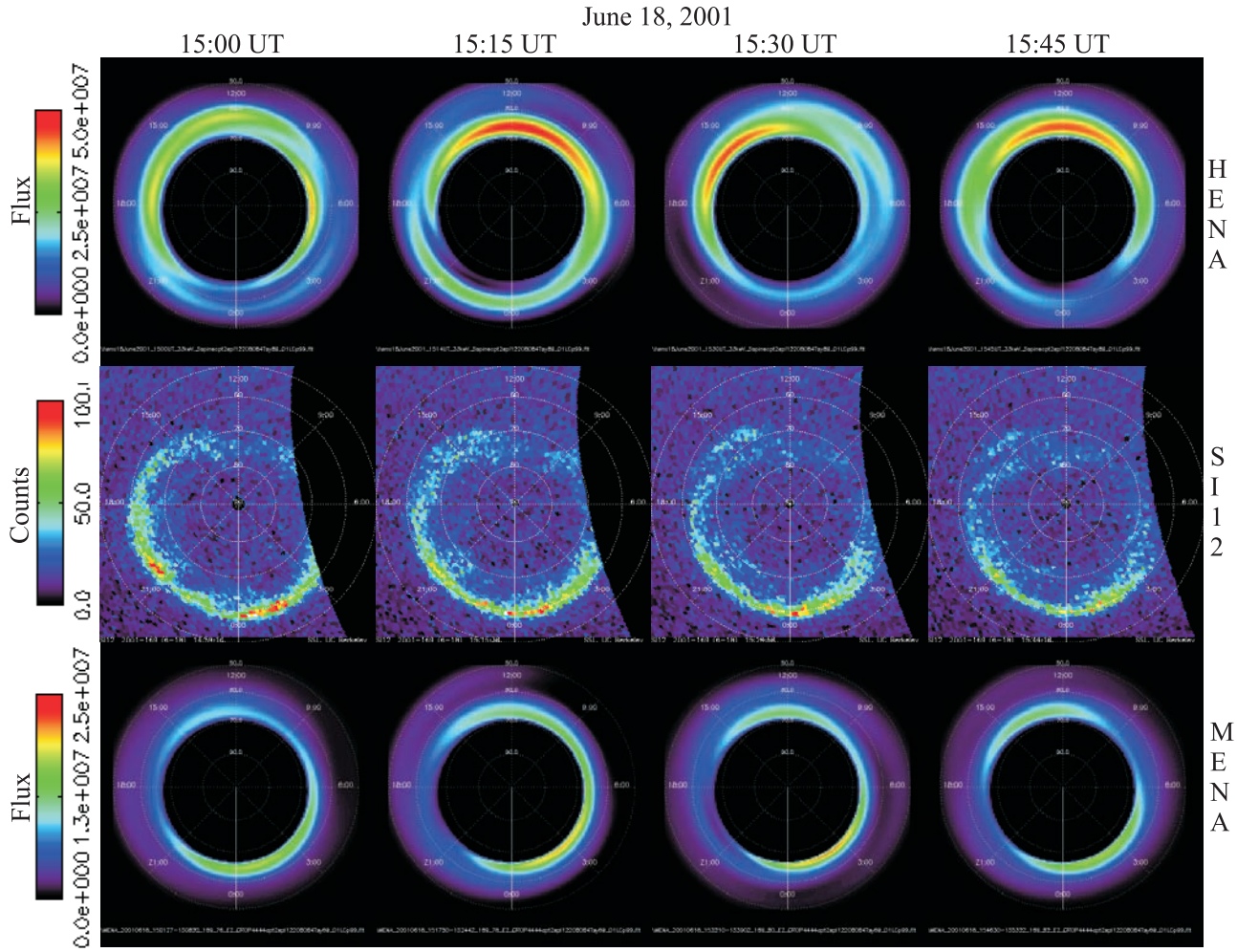

Figure 10. Images from 1500–1545 UT on 18 June 2001. Format is the same as Figure 2.

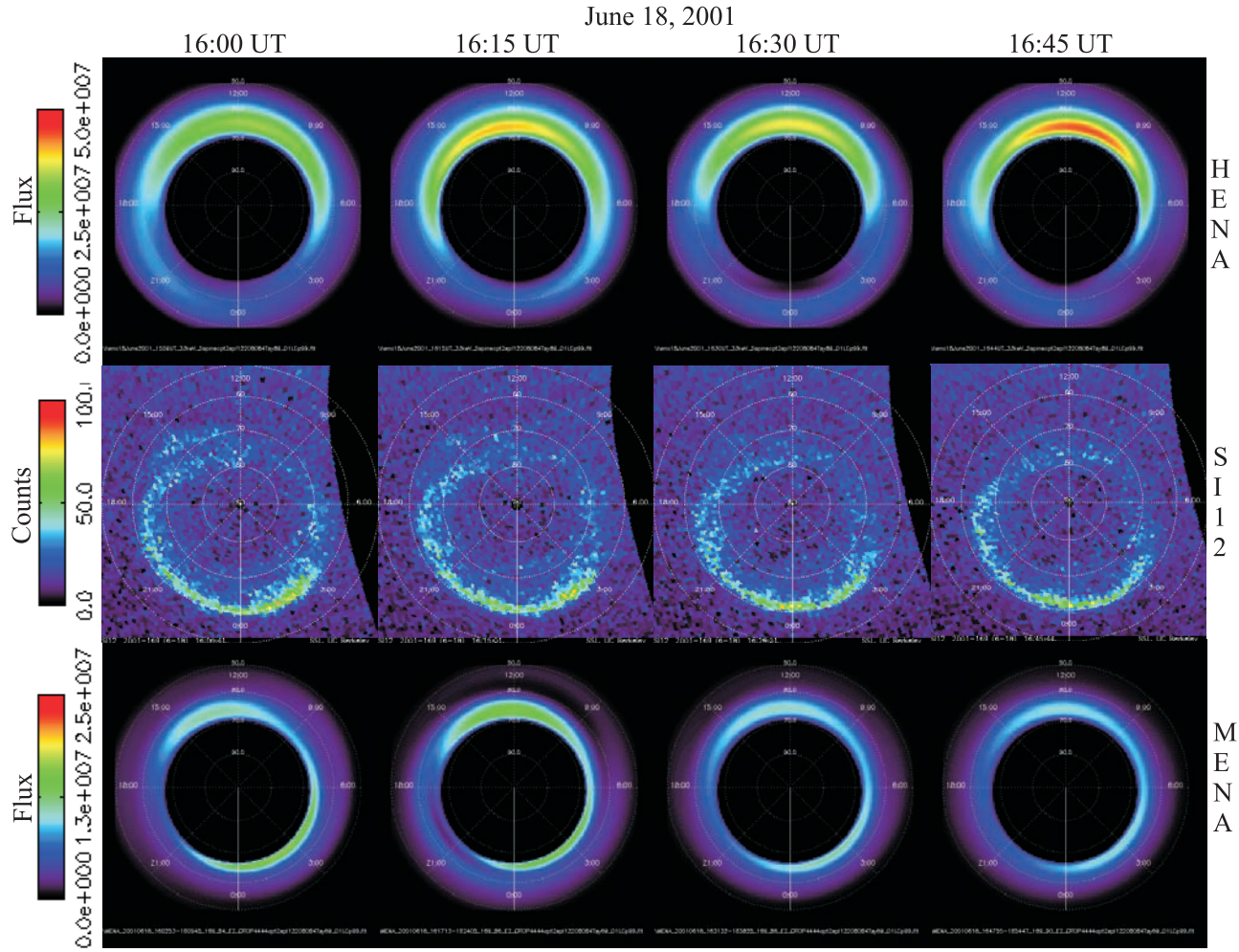

Figure 11. Images from 1600–1645 UT on 18 June 2001. Format is the same as Figure 2.

[29] *Donovan et al.* [2002] found virtually instantaneous increases in the proton auroral brightness associated with sudden increases in solar wind dynamic pressure. This was particularly true when B_z was positive. They concluded that the enhanced proton precipitation resulted from adiabatic energization and not enhanced pitch angle scattering. This mechanism, however, does not seem to be operative in the three cases treated here.

4. Summary

[30] Images of precipitating protons and trapped protons at 8.5 and 33 keV have been presented during three periods: (1) 12 August 2000 from 1000 UT to 1345 UT, just after the peak of a strong geomagnetic storm, (2) 2 June 2001 from 0000 to 0545 UT, during the main phase and initial recovery of a weak storm, and (3) 18 June 2001 from 1300 to 1645 UT, late in the recovery phase of another weak storm. Some might even quarrel with the definition of the 2 June 2001 period as a storm since SYMH does not reach −50 nT. A number of features of the precipitating trapped protons observed in these time intervals have been previously reported for other events, especially the fact that the strength of the precipitating protons and trapped protons do not correlate [*Mende et al.*, 2002b]. The principal new features are that (1) the precipitating and trapped protons occur at similar magnetic latitudes, and (2) the MLT location of the 8.5 keV trapped protons usually correlates with the location of the trapped protons, whereas the MLT location of the 33 keV trapped protons often anticorrelates. Understanding this behavior should provide stringent tests for models of the Earth's inner magnetosphere.

[31] **Acknowledgment.** Arthur Richmond thanks Finn Soraas and James Spann for their assistance in evaluating this paper.

References

Burch, J. L. (2000), IMAGE mission overview, *Space Sci. Rev.*, *91*, 1.

Burch, J. L., W. S. Lewis, T. J. Immel, P. C. Anderson, H. U. Frey, S. A. Fuselier, J.-C. Gerard, S. B. Mende, D. G. Mitchell, and M. F. Thomsen (2002), Interplanetary magnetic field control of afternoon-sector detached proton auroral arcs, *J. Geophys. Res.*, *107*(A9), 1251, doi:10.1029/2001JA007554.

Carlson, C. W., J. P. McFadden, P. Turin, D. W. Curtis, and A. Magoncelli (2001), The electron and ion plasma experiments for FAST, *Space Sci. Rev.*, *98*, 33–66.

Donovan, E., D. Knudsen, J. Wygant, M. Henderson, R. Ergun, L. Cogger, R. Pfaff, and F. Creutzberg (2002), Enhanced auroral proton and electron precipitation immediately following rapid magnetopause compressions, *Eos Trans. AGU*, *83*(47), Fall Meet. Suppl., Abstract SM72D-06.

Erlandson, R. E., and A. J. Ukhorskiy (2001), Observations of electromagnetic ion cyclotron waves during geomagnetic storms: Wave occurrence and pitch angle scattering, *J. Geophys. Res.*, *106*, 3883–3895.

Frey, H. U., S. B. Mende, T. J. Immel, S. A. Fuselier, E. S. Claflin, J.-C. Gerald, and B. Hubert (2002), Proton aurora in the cusp, *J. Geophys. Res.*, *107*(A7), 1091, doi:10.1029/2001JA900161.

Immel, T. J., S. B. Mende, H. U. Frey, L. M. Peticolas, C. W. Carlson, J.-C. Gerard, B. Hubert, S. A. Fuselier, and J. L. Burch (2002), Precipitations of auroral protons in detached arcs, *Geophys. Res. Lett.*, *29*(11), 1519, doi:10.1029/2001GL013847.

Jordanova, V. K., C. J. Farrugia, R. M. Thorne, G. V. Khazanov, G. D. Reeves, and M. F. Thomsen (2001), Modeling ring current proton precipitation by electromagnetic ion cyclotron waves during the May 14–16, 1997 storm, *J. Geophys. Res.*, *106*, 7–22.

Kozyra, J. U., V. K. Jordanova, R. B. Horne, and R. M. Thorne (1997), Modeling of the contribution of electromagnetic ion cyclotron (EMIC) waves to stormtime ring erosion, in *Magnetic Storms*, *Geophys. Monogr. Ser.*, vol. 98, edited by B. T. Tsurutani et al., p. 187, AGU, Washington, D.C.

Mende, S. B., et al. (2000), Far ultraviolet imaging from the IMAGE spacecraft, *Space Sci. Rev.*, *91*, 287.

Mende, S. B., H. U. Frey, M. Lampton, J.-C. Gerard, B. Hubert, S. Fuselier, J. Spann, R. Gladstone, and J. L. Burch (2001), Global observations of proton and electron auroras in a substorm, *Geophys. Res. Lett.*, *28*(6), 1139–1142.

Mende, S. B., H. U. Frey, C. W. Carlson, J. McFadden, J.-C. Gerard, B. Hubert, S. Fuselier, R. Gladstone, and J. L. Burch (2002a), IMAGE and FAST observations of substorm recovery phase aurora, *Geophys. Res. Lett.*, *29*(12), 1602, doi:10.1029/2001GL013027.

Mende, S. B., H. U. Frey, T. J. Immel, D. G. Mitchell, P. C:son Brandt, and J.-C. Gerard (2002b), Global comparison of magnetospheric ion fluxes and auroral precipitation during a substorm, *Geophys. Res. Lett.*, *29*(12), 1609, doi:10.1029/2001GL014143.

Mende, S. B., H. U. Frey, B. J. Morsony, and T. J. Immel (2003), Statistical behavior of proton and electron auroras during substorms, *J. Geophys. Res.*, *108*(A9), 1339, doi:10.1029/2002JA009751.

Mitchell, D. G., et al. (2000), High Energy Neutral Atom (HENA) Imager for the IMAGE mission, *Space Sci. Rev.*, *91*, 67.

Ostgaard, N., D. L. Detrick, T. J. Rosenberg, R. R. Vondrak, H. U. Frey, S. B. Mende, S. E. Haland, and J. Stadsnes (2003), High-latitude dayside energetic precipitation and IMF B_z rotations, *J. Geophys. Res.*, *108*(A4), 8013, doi:10.1029/2002JA009350.

Perez, J. D., M.-C. Fok, and T. E. Moore (2000), Deconvolution of energetic neutral atom images of the Earth's magnetosphere, *Space Sci. Rev.*, *91*, 421.

Perez, J. D., G. Kozlowski, P. C:son Brandt, D. G. Mitchell, J.-M. Jahn, C. J. Pollock, and X.-X. Zhang (2001), Initial ion equatorial pitch angle distributions from medium and high energy neutral atom images obtained by IMAGE, *Geophys. Res. Lett.*, *28*, 1155.

Perez, J. D., X.-X. Zhang, P. C:son Brandt, D. G. Mitchell, J.-M. Jahn, and C. J. Pollock (2004), Dynamics of ring current ions as obtained from IMAGE HENA and MENA ENA images, *J. Geophys. Res.*, *109*, A05208, doi:10.1029/2003JA010164.

Pollock, C. J., et al. (2000), Medium Energy Neutral Atom (MENA) Imager for the IMAGE mission, *Space Sci. Rev.*, *91*, 113.

Sóraas, F., K. Aarsnes, J. A. Lundblad, and D. S. Evans (1999), Enhanced pitch angle scattering of protons at mid-latitudes during geomagnetic storms, *Phys. Chem. Earth, Part C*, *24*, 287.

Tsyganenko, N. A. (1989), A magnetospheric magnetic field model with a warped tail current sheet, *Planet. Space Sci.*, *37*, 5.

Yahnin, A. G., T. A. Yahnina, N. Y. Ganushkina, V. Angelopoulos, F. S. Mozer, J. Kangas, J. Manninen, T. A. Fritz, C. T. Russell, and M. F. Thomsen (2002), Multi-satellite study of phenomena in the evening magnetosphere during the Pc1-2 event, in *Physics of Auroral Phenomena, Proceedings of XXV Annual Seminar, Apatity*, pp. 85–88, Kola Sci. Cent., Russian Acad. of Sci., Moscow.

P. C:son Brandt and D. G. Mitchell, Applied Physics Laboratory, Johns Hopkins University, Laurel, MD 20723, USA. (brandpc1@jhuapl.edu; donald.g.mitchell@jhuapl.edu)

J.-M. Jahn and C. J. Pollock, Space Science Department, Southwest Research Institute, 6220 Culebra Road, San Antonio, TX 78238-5166, USA. (jjahn@swri.edu; cpollock@swri.edu)

S. B. Mende, Space Science Laboratory, University of California, Berkeley, 7 Gauss Way, Berkeley, CA 94720, USA. (mende@ssl.berkeley.edu)

J. D. Perez and X.-X. Zhang, Physics Department, Auburn University, AL 36849, USA. (perez@physics.auburn.edu; zhangx@cspar.uah.edu)